FIGURES FOR ADVANCED ALGEBRAIC TOPOLOGY LECTURE NOTES

(***Lecture notes link:*** http://math.ucr.edu/~res/math246A–2012/advancednotes2012.pdf)

I : Foundational and geometric background

I.0 : Review

Barycentric coordinates. In the drawing below, each of the points **P, Q, R** lies in the plane determined by $\mathbf{P_1}$, $\mathbf{P_2}$, and $\mathbf{P_3}$, and consequently each can be written as a linear combination $w_1\mathbf{P_1} + w_2\mathbf{P_2} + w_3\mathbf{P_3}$, where $w_1 + w_2 + w_3 = 1$. For the point **P**, the barycentric coordinates w_i are all positive, while for the point **R** the barycentric coordinates are such that $w_1 = 0$ but the other two are positive, and for the point **Q** the barycentric coordinates are such that w_1 is negative but the other two are positive.

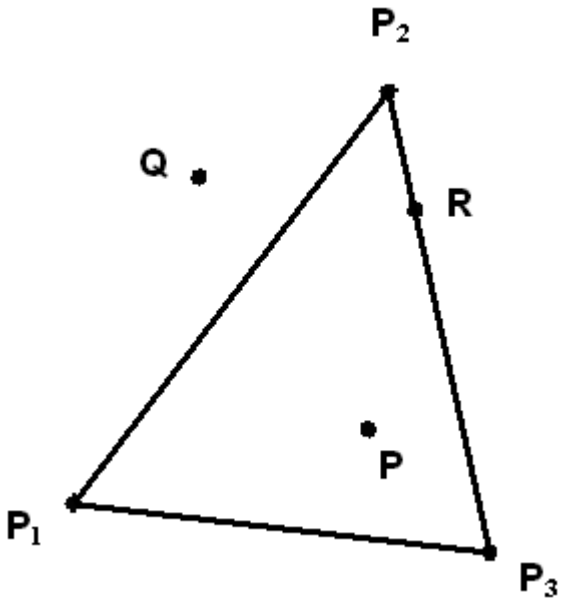

FIGURE I.0.1

(***Source:*** http://graphics.idav.ucdavis.edu/education/GraphicsNotes/Barycentric-Coordinates/Barycentric-Coordinates.html)

Examples of points for which w_2 is positive but the remaining coordinates are negative can also be constructed using this picture; for example, if one takes the midpoint **M** of the segment $[\mathbf{P_1P_3}]$, then the point $\mathbf{S} = 2\mathbf{P_2} - \mathbf{M}$ has this property (geometrically, $\mathbf{P_2}$ is the midpoint of the segment joining **M** and **S**).

Illustration of a 2 – simplex . We shall use a modified version of Figure **1;** the points of the **2 –** simplex with vertices $\mathbf{P_1}$, $\mathbf{P_2}$, and $\mathbf{P_3}$ consists of the triangle determined by these points and the points which lie inside this triangle (in the usual intuitive sense of the word)**.**

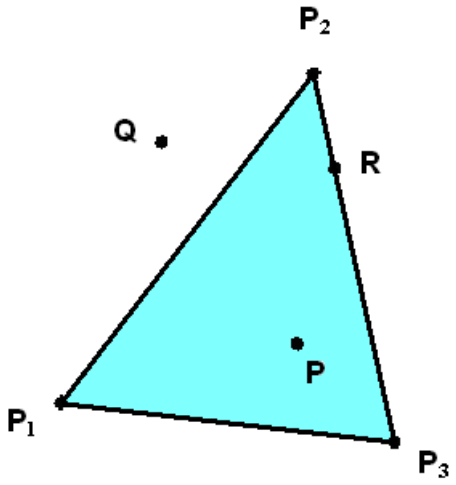

FIGURE I.0.2

In this picture the points **P** and **R** lie on the simplex $\mathbf{P_1P_2P_3}$ because their barycentric coordinates are all nonnegative**,** but the point **Q** does not because one of its barycentric coordinates is negative**.**

Note that the **(*proper*) *faces*** of this simplex are the closed segments $\mathbf{P_1P_2}$**,** $\mathbf{P_2P_3}$**,** and $\mathbf{P_1P_3}$ joining pairs of vertices as well as the three vertices themselves (and possibly the empty set if we want to talk about an empty face with no vertices)**.**

Simplicial decompositions. It is useful to look at a few spaces given as unions of **2 –** simplices**,** some of which determine simplicial complexes in the sense of the notes and others that do not**.**

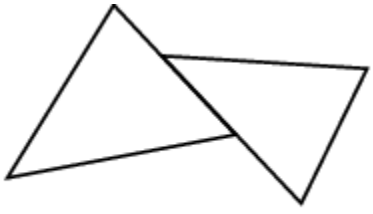

not a simplicial complex

FIGURE I.0.3

(*Source:* http://mathworld.wolfram.com/SimplicialComplex.html)

In the example above the intersection of the **2 –** simplices is not a common face**.** On the other hand**,** we can split the two simplices into smaller pieces such that we do have a simplicial decomposition**.**

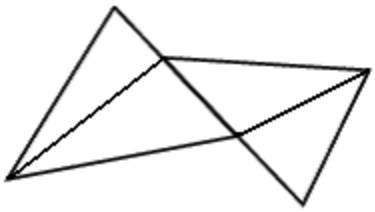

simplicial complex

FIGURE I.0.4

Here are two more examples; in the second case the simplices determine a simplicial complex and in the first they do not. As in the preceding example, one can subdivide the simplices in the first example to obtain a simplicial decomposition.

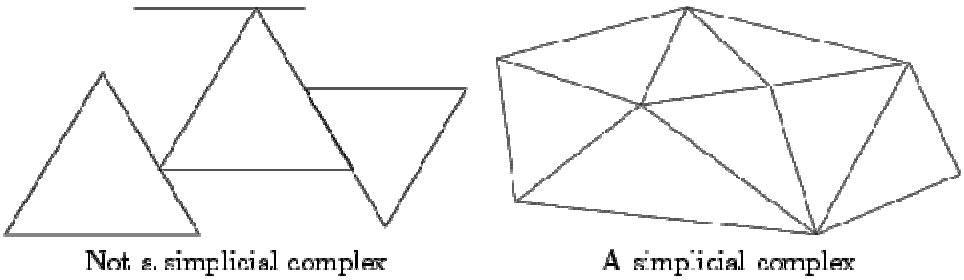

(***Source:*** http://planning.cs.uiuc.edu/node274.html)

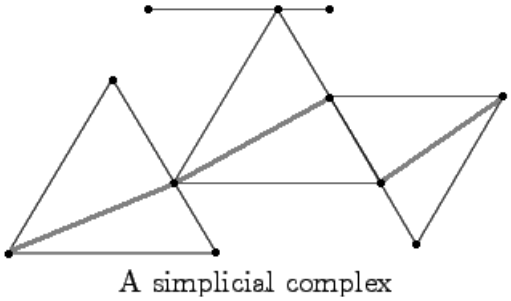

FIGURE I.0.5

Triangulations. One cam split the annulus bounded by two circles into four isometric pieces as in the drawing on the next page.

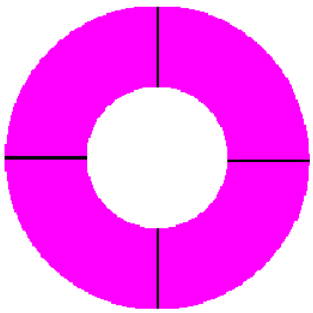

FIGURE I.0.6

Each of the four pieces is homeomorphic to a solid rectangle. Since a solid rectangle has a simplicial decomposition into two $2-$ simplices, one can use such a decomposition to form a triangulation of the solid annulus.

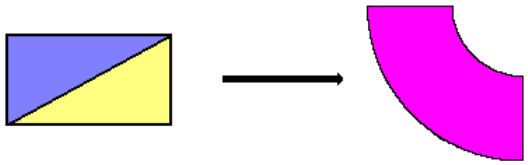

FIGURE I.0.7

A closely related way of triangulating the annulus is suggested by the figure below:

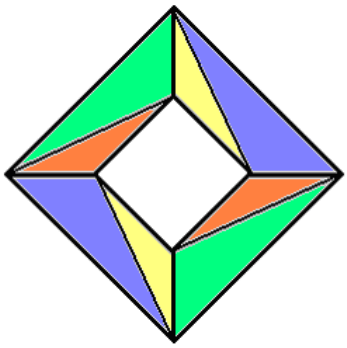

FIGURE I.0.8

Similarly, many familiar closed polygonal regions can be triangulated fairly easily. Here is an example for a solid hexagon.

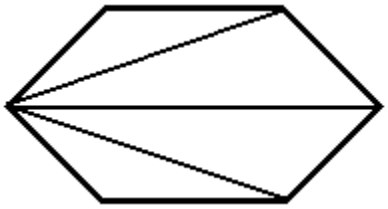

FIGURE I.0.9

Triangulations of prisms. The drawings below illustrate the standard decomposition of a $3-$ dimensional triangular prism.

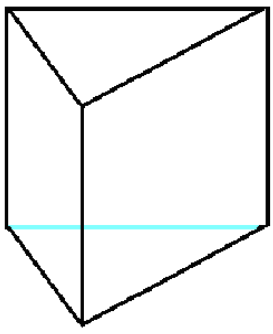

FIGURE I.0.10

If we take x_0, x_1, and x_2 to be the vertices of the bottom triangle and y_0, y_1, and y_2 to be the vertices of the top triangle, then the decomposition is given as follows:

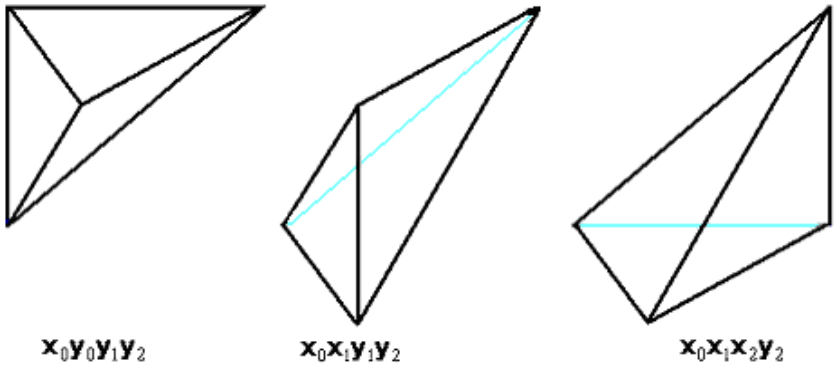

FIGURE I.0.11

I.1 : Ordered simplicial chains

Star shaped complexes. The following drawing of an eight pointed star depicts a simplicial complex which is star shaped with respect to the vertex in the center. Note that the complex is not star shaped with respect to any of the other vertices. In contrast, a simplex with the standard face decomposition is star shaped with respect to each of its vertices. Two 2 – simplices in the plane with a common edge are an example of a complex which is star shaped with respect to exactly two vertices (and not star shaped with respect to the other two).

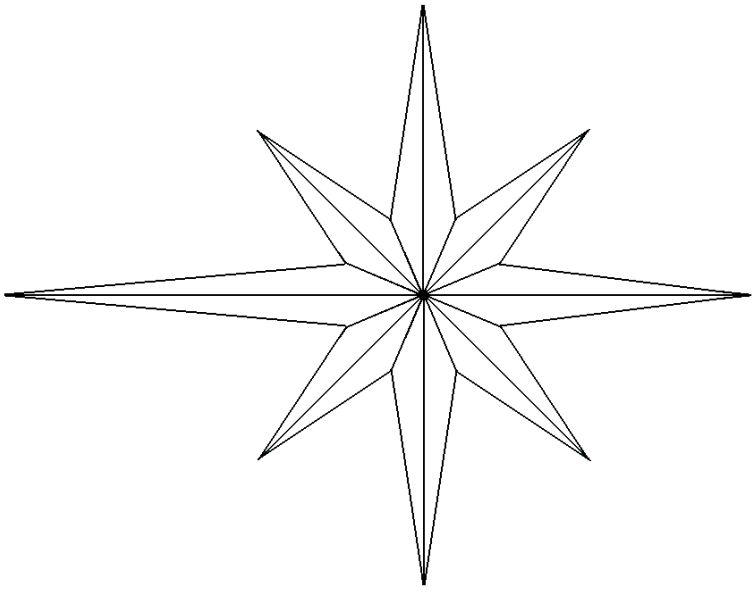

FIGURE I.1.1

(***Source:*** http://www.ezartsncrafts.com/templates/8star.gif)

I.2 : Subdivisions

Simple subdivisions 1. The drawing below depicts a subdivision of a $1-$ simplex given by a closed interval in the real line into three $1-$ simplices (which are just subintervals of the original interval).

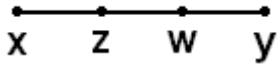

FIGURE I.2.1

Similarly, every partition of an interval determines a subdivision.

Simple subdivisions 2. The drawing below depicts a subdivision of a $2-$ simplex into two $2-$ simplices.

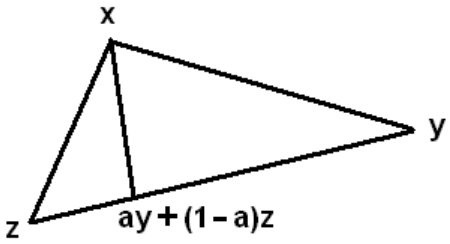

FIGURE I.2.2

If $\mathbf{w} = a\mathbf{y} + (1-a)\mathbf{z}$ where $0 < a < 1$ and $p\mathbf{x} + q\mathbf{y} + r\mathbf{z}$ is a point on the simplex **xyz** (so that $p, q, r \geq 0$ and $p\mathbf{x} + q\mathbf{y} + r\mathbf{z} = 1$), then the point $p\mathbf{x} + q\mathbf{y} + r\mathbf{z}$ lies on the simplex **xwz** if and only if $p = 1$ or $p < 1$ and $q \geq a(1-p)$, and $p\mathbf{x} + q\mathbf{y} + r\mathbf{z}$ lies on the simplex **xwy** if and only if $p = 1$ or $p < 1$ and $q \leq a(1-p)$. The intersection of these simplices is the face with vertices **x** and **w**. Some other simple subdivisions of a $2-$ simplex are illustrated below.

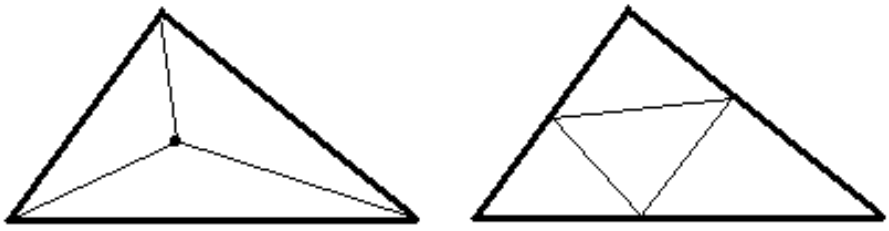

FIGURE I.2.3

A nonexample. In general, if we given two simplicial decompositions, then neither is a subdivision of the other. For example, neither of the two simplicial decompositions of a rectangle described below is a subdivision of the other.

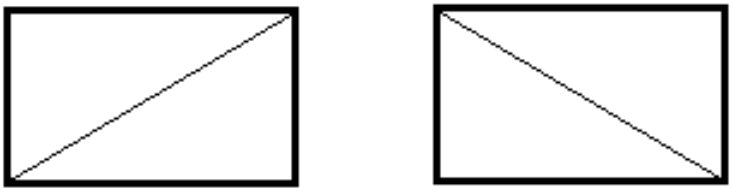

FIGURE I.2.4

On the other hand, there is a decomposition which is a subdivision of ***both*** the decompositions shown above.

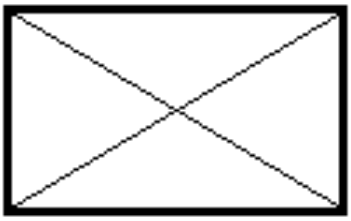

FIGURE I.2.5

More generally, if we are given two simplicial decompositions $\mathbf{K}$ and $\mathbf{L}$ of a polyhedron **P** then one can ***always*** construct a third decomposition which is a subdivision of both $\mathbf{K}$ and $\mathbf{L}$. This follows from results in the book, ***Elementary Differential Topology,*** by J. R. Munkres (see the notes for a more complete citation).

Here is a slightly more complicated pair of examples:

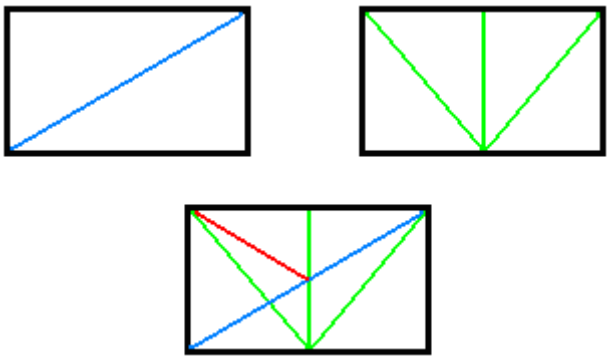

FIGURE I.2.6

Examples from the previous section. Here are illustrations to indicate how one can subdivide the nonsimplicial decompositions from the figures in Section $\mathbf{I.2}$ to obtain simplicial decompositions.

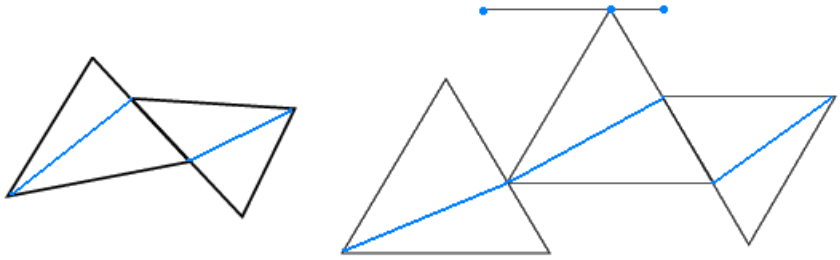

FIGURE I.2.7

Barycentric subdivisions. Here is a drawing to illustrate the barycentric subdivision of a 2 – simplex.

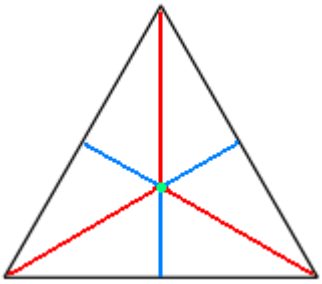

FIGURE I.2.8

The vertices of a 2 – simplex in this subdivision are given by **a, b** and **c,** where **a** is a vertex of the original simplex**, b** is the midpoint of an edge which has **a** as a vertex**,** and **c** is the barycenter of the 2 – simplex itself. In this example**,** the diameters of the 2 – simplices in the barycentric subdivision are $2/3$ the diameter of the original simplex**.**

The drawing below illustrates the barycentric subdivision of a solid rectangular region with its basic decomposition into two 2 – simplices along a diagonal**.** Observe that the decompositions of the top and bottom 2 – simplices are just the barycentric subdivisions of the latter**,** and the decomposition of the edge where they intersect is just the barycentric subdivision of that edge**.**

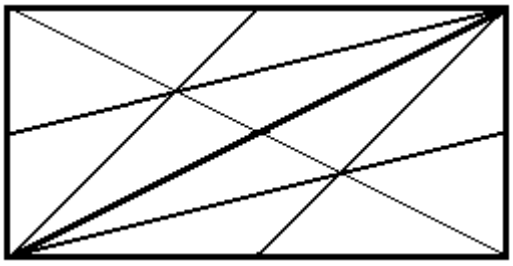

FIGURE I.2.9

The next drawing illustrates the ***second barycentric subdivision*** of a 2 – simplex (however**,** the locations of several vertices are slightly inaccurate)**.**

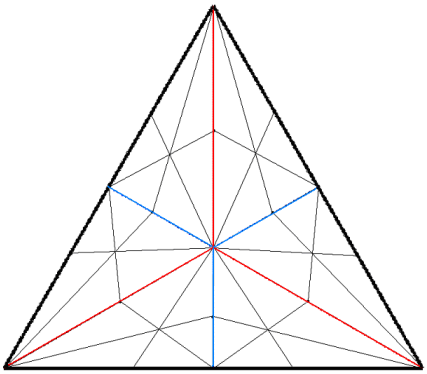

FIGURE I.2.10

This decomposition of the **2 –** simplex has **25** vertices**, 60** edges and **36** simplices that are **2 –** dimensional**.** Incidentally**,** in the third barycentric subdivision there are **121** vertices**, 336** edges and **216** simplices that are **2 –** dimensional**.**

Final comment on barycentric subdivisions. In the proof that the barycentric subdivision actually defines a simplicial decomposition of a simplex**,** the simplex containing a given point is determined by putting the barycentric coordinates in linear order**.** The drawing below indicates the correspondence between inequality chains and **2 –** simplices in the barycentric subdivision of a **2 –** simplex**.**

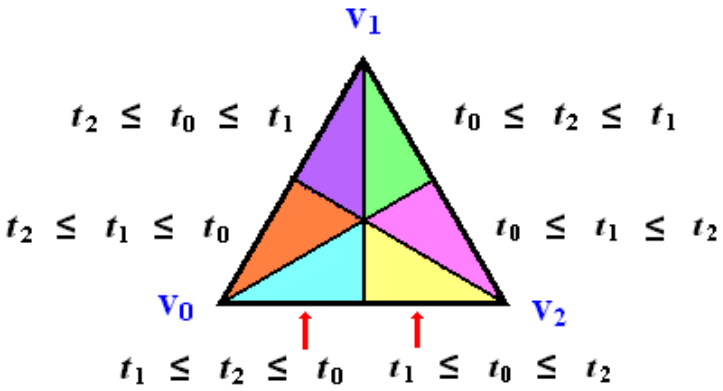

FIGURE I.2.11

I.3 : Abstract cell complexes

The Königsberg Bridge Network. In the 18th century**,** the city of Königsberg (now known as Kaliningrad**,** on the Baltic Sea in a small sliver of Russian territory sandwiched between Poland and Lithuania) had seven bridges across the Pregel (or Pregolya) River**,** which runs through the city**.**

(***Source:*** http://news.bbc.co.uk/2/hi/europe/country_profiles/6177003.stm)

The original question was to find a path through the city which crosses over each of these seven bridges exactly once, and Euler reduced the problem to a question about an edge – vertex graph; specifically, one first eliminates all features but the land masses and the bridges connecting them, and then one represents each land mass with a vertex and each bridge with an edge whose endpoints are the two land masses it connects.

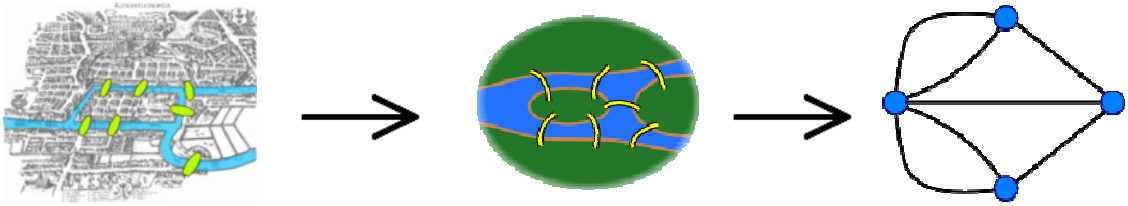

(***Source:*** http://en.wikipedia.org/wiki/Seven_Bridges_of_K%C3%B6nigsberg)

In **1736** Euler proved that it was impossible to find a path of the desired type, and a description of his approach in modern terminology appears in the online **205B** notes.

Cell attachments and NDR neighborhoods. The drawing below represents a space **X** obtained by taking another space **A** and attaching a single **2 –** cell. The subspace **A** is colored in a peach – like shade of orange, and the blue and yellow regions correspond to the cell. In this case **A** is a strong deformation retract of the open set **U** given by **A** together with the regions colored in medium and light blue with the frontier points on the boundary circle removed. Furthermore, **U** of has a subneighborhood **V** (namely, the union of **A** and the region colored in medium blue) such (1) that the closure of **V** is contained in **U**, and (2) **A** is a strong deformation retract of both **V** and its closure. Of course, the details are in the notes.

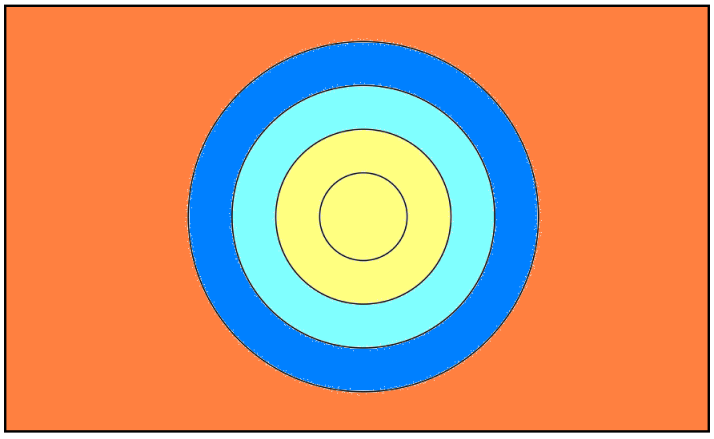

More generally, if **A** is a subset of **X** such that **A** is a strong deformation retract of some open neighborhood **U** of **A** in **X**, then one frequently says that **A** is a ***neighborhood deformation retract*** (***NDR***) in **X.** An extremely large (probably dominant) share of the subspaces studied in topology and geometry have this propery (in particular, this is true for subcomplexes of a simplicial complex, smooth submanifolds of a smooth manifold, and subsets of Euclidean space defined by finitely many polynomial equations and/or inequalities), and their properties are discussed further in the following reference:

> **N. E. Steenrod**, *A convenient category of topological spaces*. Michigan Mathematical Journal **14** (1967), pp. 133 – 152.

I.4 : The Homotopy Extension Property

The standard models. The crucial point in the proof of the Homotopy Extension Property is that the inclusion of $D^n \times [0,1] \cup S^{n-1} \times [0,1]$ in the cylinder $D^n \times [0,1]$ is a retraction; an illustration of this retraction when $n = 1$ is given below:

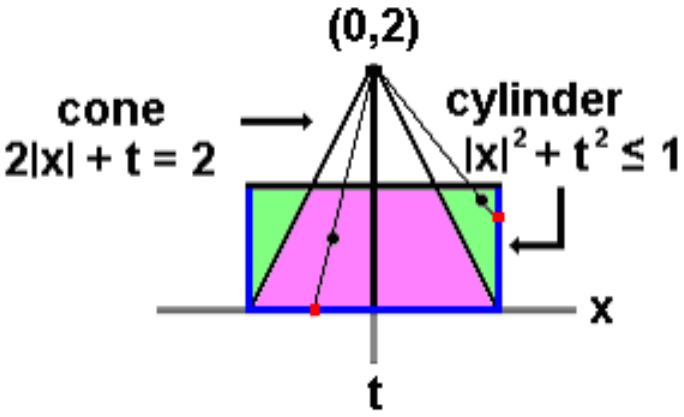

In this illustration, the retraction sends the points marked in black into the points marked in red on the corresponding lines. The explicit definition of the retraction has two cases, depending upon whether or not the original point lie in the pink colored region or the green colored region(s).

One can obtain the case $n = 2$ from the one – dimensional case by taking solids and surfaces of revolution about the t – axis, and likewise in higher dimensions one can view the drawing as a planar cross section of the general construction.

I.6 : Cones and suspensions

Cones. In the simplest cases, Proposition 1 implies that the topological cones on spaces are canonically homeomorphic to the standard cones of elementary geometry. For example, if **X** is the circle S^1, then Proposition 1 shows that the cone on **X** is

homeomorphic to the lateral (or top) surface of the cone illustrated below, and if **X** is the disk $\mathbf{D}^2$, then Proposition **1** shows that the cone on **X** is homeomorphic to the solid cone.

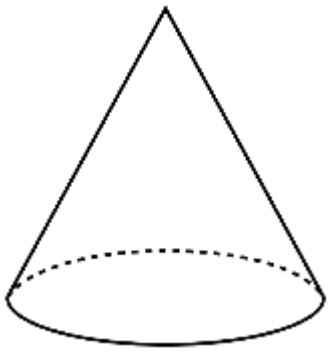

FIGURE I.6.1

In this drawing, the original space is the base of the cone and the point at the top corresponds to the equivalence class of the subspace which is collapsed to a point.

Suspensions. The drawing below illustrates the suspension of the circle. Note that the closure of the piece above the $xy-$ plane is merely the cone on the circle, while the closure of the piece below the $xy-$ plane is the mirror image of that cone with respect to reflection about the $xy-$ plane. Frequently these two subspaces are denoted by the symbols like $\mathbf{C}_+(\mathbf{X})$ and $\mathbf{C}_-(\mathbf{X})$.

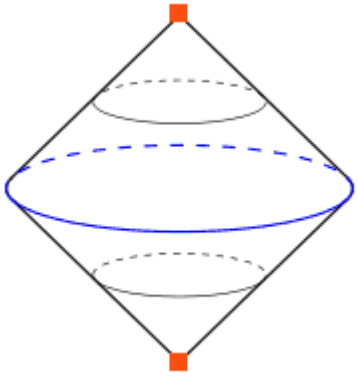

(See the Wikipedia citation in **http://www.answers.com/topic/suspension**)

FIGURE I.6.2

In this drawing, the original space is outlined in blue, and the collapsed end points (the "poles") are both in deep orange.

II : Construction and uniqueness of singular homology

II . 1 : Definitions and basic properties

Approximating spaces by polyhedra. If **X** is a compact subset of the plane, then **X** is an intersection of subspaces which are homeomorphic to polyhedra. The drawing below illustrates this for a subspace called the ***Hawaiian earring.*** In coordinates this space is the union of the circles tangent to the origin with centers $(1/2^k, 0)$ where ***k*** runs through all nonnegative integers.

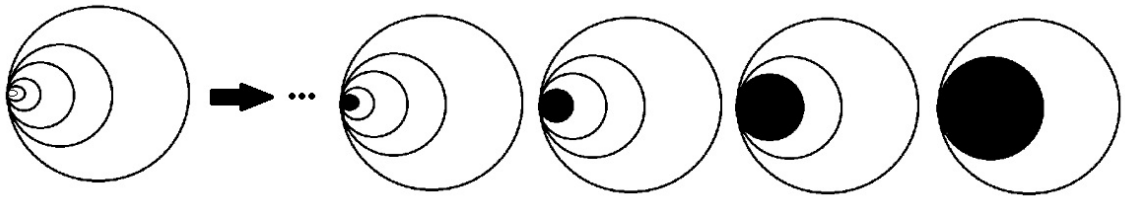

In the drawing, the Hawaiian earring is the space at the left, and it is the intersection of the spaces $\mathbf{X}_k$, where $\mathbf{X}_k$ is formed by adding the disk centered at $(1/2^k, 0)$. Note that each of these sets $\mathbf{X}_k$ is homeomorphic to a polyhedron. The **Čech homology theory** described in Section **III.5** of these notes is related to such approximations.

In contrast, **singular homology theory** is based upon the idea that every open subset of the plane is an increasing union of polyhedra. For example, in the drawings below consider the region **U** bounded by the red ellipse. For each ***k***, let $\mathbf{P}_k$ be the polyhedron which is a union of solid squares which are contained in **U** and whose vertices are rational numbers whose denominators are divisible by 2^k. Then standard results in measure theory imply that **U** is the union of the sets $\mathbf{P}_k$. The drawings below show three successive approximations to **U** by such configurations of solid squares and highlight the solid squares that are added at each step.

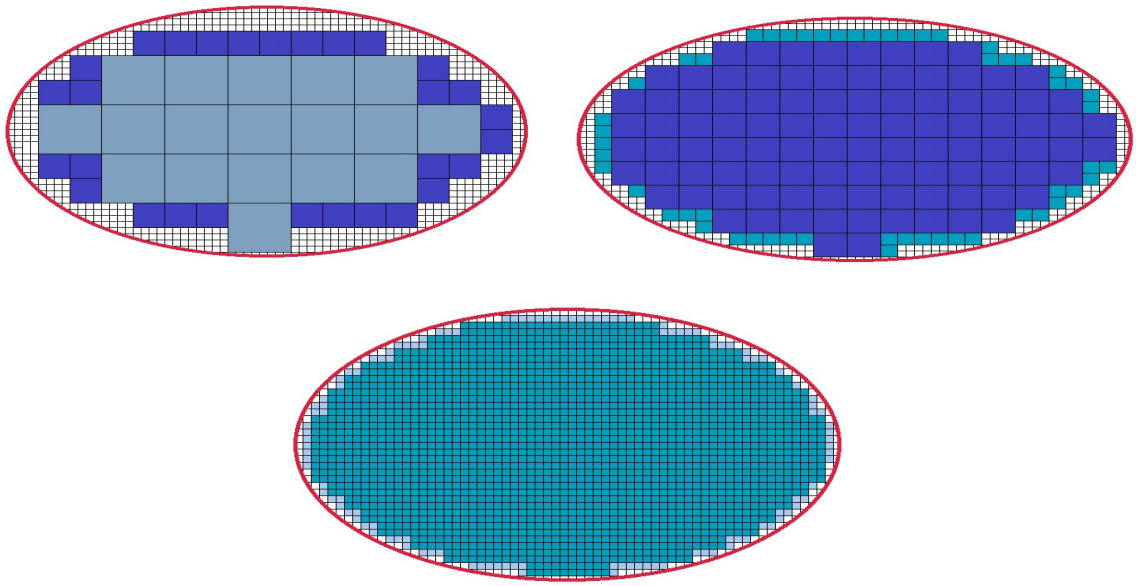

For more general spaces, it is useful to think of singular homology as an approach to studying the homology of a space by trying to construct polyhedral which somehow approximate the original space. The results of **205B** show that covering space theory does not work well for some exotic examples of spaces, and the same is true for singular homology. However, there is a large class of spaces (including topological manifolds) for which singular homology theory gives the "right" homology groups.

II . 3 : Excision and Mayer – Vietoris sequences

Excision for polyhedral in simplicial homology. Here is a drawing:

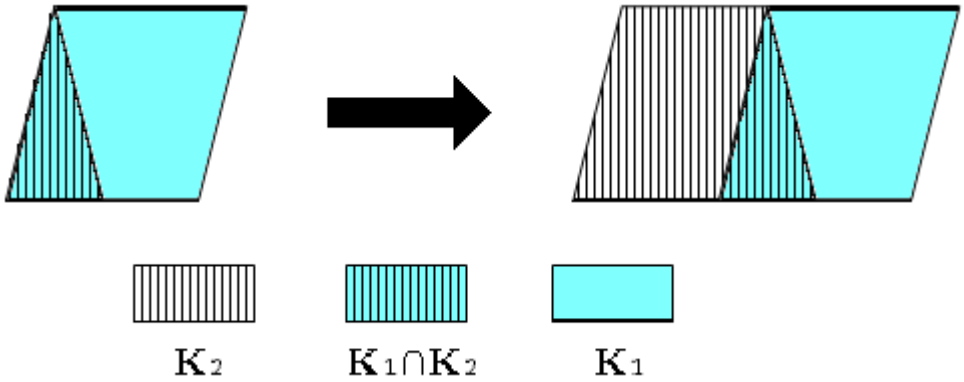

The inclusion map of pairs induces isomorphisms in simplicial homology. In this drawing K_2 is striped, K_1 is colored, and their intersection is both.

Excision in singular homology. Here is a drawing:

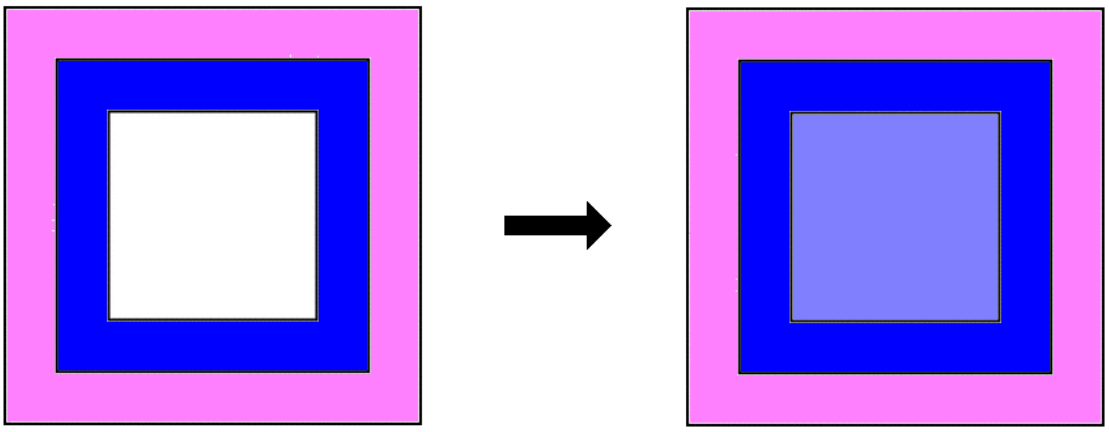

In this case the inclusion map of pairs induces isomorphisms in singular homology; the excised subset U corresponds to the smallest square in the middle of X.

Common feature. In both cases we have continuous mappings of pairs f from (Y, B) to (X, A) which maps $Y - B$ homemorphically to $X - A$ (such a map is often called a ***relative homeomorphism***). **Many,** but definitely **not all,** relative homeomorphisms induce isomorphisms in singular homology**.**

How to find counterexamples as described in the preceding statement. If relative homeomorphisms always induced isomorphisms in singular homology when the subsets A and B are closed in X and Y respectively**,** then one would have Mayer – Vietoris exact sequences for spaces given as the union of closed subpsaces (this can be derived as in the first chapter of Eilenberg and Steenrod)**,** but later in the notes we shall prove that this is not the case**.**

II . 5 : Polyhedral generation, direct limits and uniqueness

Additional examples of Hatcher Δ – complexes. The right hand figure represents a complex obtained from the **2 –** simplex on the left by identifying two side edges**.**

A second example can be constructed from this by identifying the vertex at the bottom with the (unique) vertex at the top**.** The original example has two vertices**,** two edges and one face**,** and the second example has one vertex**,** two edges and one face**.** As indicated on page **54** of the notes**,** an exercise in Hatcher implies that the second barycentric subdivisions of both complexes are homeomorphic to polyhedra**.**

V : Cohomology and Differential Forms

V . 4 : De Rham's Theorem

The following drawing is designed to illustrate the decomposition of an open set $\mathbf{U}$ in Theorem **2** of the notes. We are given a presentation of the open set as a union of compact subsets $\mathbf{K_i}$, each of which is contained in the interior of the next one in the sequence. The sets $\mathbf{A_i}$, which correspond to the colored bands, are obtained by removing the interior of $\mathbf{K_{i-1}}$ from $\mathbf{K_i}$

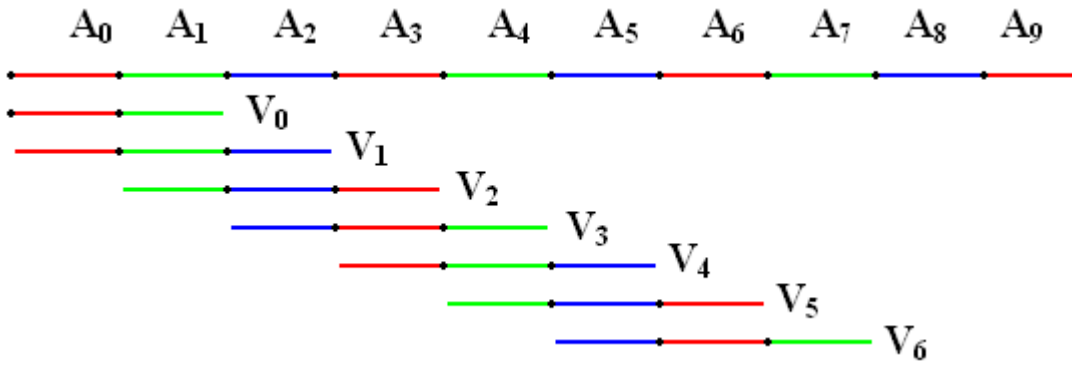

The sets $\mathbf{V_i}$ are open neighborhoods of the sets $\mathbf{A_i}$, and they are constructed so that $\mathbf{V_i}$ and $\mathbf{V_j}$ have points in common only if $|\mathbf{i - j}|$ is at most **2**. In the proof of Theorem **2** one uses these sets to find smaller open neighborhoods $\mathbf{W_i}$ of $\mathbf{A_i}$ such that $\mathbf{W_i}$ is contained in $\mathbf{V_i}$ and $\mathbf{W_i}$ is a finite union of open disks. Thus the families

$$\{\mathbf{W_0, W_3, W_6, \ldots}\} \quad \{\mathbf{W_1, W_4, W_7, \ldots}\} \quad \{\mathbf{W_2, W_5, W_8, \ldots}\}$$

consist of pairwise disjoint open subsets, each of which is a finite union of convex open subsets. We know that de Rham's Theorem holds for each $\mathbf{W_i}$ by previous results in the notes, and Proposition **3** implies that the theorem also holds for the unions $\mathbf{G_0}$, $\mathbf{G_1}$, $\mathbf{G_2}$ of the open sets in each of the three families. Theorem **4** gives the final steps to showing that de Rham's Theorem is true for finite unions of these sets $\mathbf{G_i}$ and hence is true for the arbitrary open subset $\mathbf{U}$ that we are considering.